# Ion Pair Amphiphile: A Neoteric Substitute that Modulates the Physico-Chemical Properties of Biomemetic Membranes

**Abstract:** Ion-pair-amphiphiles (IPAs) are neoteric pseudo double tailed compounds with potentials as novel substitute of phospholipid. IPA, synthesized by stoichiometric mixing of aqueous solution of hexadecyltrimethylammonium bromide (HTMAB) and sodium dodecyl sulphate (SDS) was used as potential substituent of naturally occurring phospholipids, soylecithin (SLC). SLC and IPA were mixed in different mole ratio along with 30 mol% cholesterol to produce stable vesicle dispersion. Cholesterol, being interdigited into the bilayer, controls the rigidity or fluidity of the membrane. Impacts of IPA on different SLC+IPA vesicles were firstly examined by monolayer studies by way of surface pressure ($\pi$) – area (A) measurements. Associated thermodynamic parameters were evaluated and the miscibility between the components was dependent on the ratio of SLC and IPA. Solution behaviour of the bilayer, in the form of vesicles, were investigated by monitoring the hydrodynamic diameter, zeta potential and polydispersity index over a period of 100 days. Systems comprising 20 and 40 mol% IPA exhibited anomalous behaviour. Thermal behaviours of the vesicles, as scrutinized by differential scanning calorimetry were correlated with the hydrocarbon chain as well as the head group packing. Steady state fluorescence spectroscopy and anisotropy analyses further supported the DSC results. Entrapment efficiency (E.E.) of the vesicles towards the cationic dye methylene blue (MB) was also evaluated. Vesicles were smart enough to entrap dye and the efficiency was found to vary with IPA concentration and the E.E. was found to be well above 80% for some stable

dispersions. Morphological behaviours of the vesicles were documented by TEM measurement and the results were well correlated with DLS study.

## 1. Introduction

Intracellular components are compartmentalized by thin bio membranes which commonly behave like a physical boundary to separate the respective compartments from the surrounding continuous environments.[1] Biological cells are directly responsible for numerous physico-chemical processes that depend on the composition of the membrane bilayer. Researches on the biological and biomemitc membranes resulted in the generation of substantial useful information in order to understand its subtle structure and its relevance in physiological environments. Bio membranes have diversity in potential because of the functional interface; it can bind to DNA, peptides, control the enzymes, *etc*.[2,3] Further researches on the membranous components suggest that bio membranes can actively play role in biochemical processes, *e.g.,* adhesion, signalling, controlling the $Na^+$/ $K^+$ balance, fusion, *etc.*[4] The resultant activity or potential of bio membranes largely depends on their components (phospholipids, cholesterol and regulatory protein, *etc*.).

The major components of the cell membranes are phospholipids that are capable to form vesicles spontaneously when they are hydrated.[5] Because of their amphiphilic nature, naturally occurring phospholipids are widely used in the synthetic formulation of vesicles in order to have further insight into their different physico-chemical properties. Researches on biomemetic membranes over the past few decades have revealed its potential application towards drug delivery, gene therapy, DNA transfection, *etc.*[6] Drug caring capabilities arise because of its unique hydrophilic and hydrophobic charisma. So last few years, vesicles have been the subject of focus for its biocompatibility and stability.

Stability of the vesicles are highly dependent on the amphiphile composition, surface charge (zeta potential) and hydrodynamic size.[7] Additionally 'rigidity' and 'fluidity' of the membranes' micro-environment also play a crucial role for its stability as they are highly dependent on the nature of the phospholipids and cholesterol. Cholesterol is one of the key components of the cell membranes as it can judiciously control the fluidity and rigidity of the bilayer.[8] Unsaturated phospholipids from natural sources, like palmitooleylphosphatidylcholine (POPC) forms less stable fluidic and permeable bilayers, whereas saturated phospholipids, *viz*., dipalmitoylphasphotidylcholine (DPPC), dimyristylphosphatidylcholine (DMPC) can form rather stable, however, rigid bilayers.[9] It is reported that vesicles comprising naturally occurring phospholipids exhibit poor stability at normal condition.[10] However strategies have been adapted by researchers in order to improve the stability of vesicles for its better performance.

Vesicles comprising different types of phospholipids have been the research of interest for past few decades.[7,11,12] Double tail and single tail surfactants which also form self-assembled structures were also introduced to produce stable vesicles dispersion. Kaler *et al*.[13] first reported about a neoteric phospholipid mimic amphiphile, which spontaneously form vesicles. This was synthesized from single chain mixed cationic and anionic surfactants, known as ion pair amphiphile (IPA). Vesicles comprising catanionic surfactants, also known as catanosomes, find its excellence for drug delivery,[6] binding with DNA,[14,15] nanoparticle synthesis[15,16] *etc*. Easy laboratory preparation of IPA marked its implication in membrane mimetic studies. However the impact of IPA on naturally occurring phospholipids (unsaturated) on monolayer and consequently on the bilayer needs some extra attention as it may produce stable vesicular dispersion for drug delivery. Such studies could shed further light on the possible yet unexplored application potentials as well as from the understanding of the fundamentals on the membranous interfaces.

In our present set of experiments, we choose to formulate stable vesicular dispersion with soylecithin (SLC) and IPA (prepared by equimolar mixing of HTMAB and SDS) with overall 30 mol% cholesterol in physiological buffer, phosphate buffer solution (PBS, pH 7.4). Formulations were prepared by varying the molar ratio of SLC and IPA. Cholesterol, which is a key component of bilayers, regulates the rigidity and fluidity of the membrane.[17] The effect of IPA on SLC in the form of monomolecular film was investigated by Langmuir monolayer technique (surface pressure – area isotherms). Bilayer, in the form of vesicles, could be viewed as the superimposition of two monolayers, so thorough study of monolayer could explain the nature of interaction between SLC and IPA. Ideality/non ideality in mixing, film compressibility and associated thermodynamic parameters were evaluated from such studies. Hydrodynamic size ($d_h$), zeta potential (Z. P.) and ploydispersity index (PDI) of the vesicles were measured by dynamic light scattering (DLS) technique. Thermotropic behavior of the bilayer was scrutinized by differential scanning calorimetry (DSC). Such studies helped in evaluating the chain melting of mixed acyl chains of SLC+IPA. Additionally, formation and deformation of water overlayer surrounding the lipidic head groups were confirmed from such study and could well be correlated with the composition of (molar ratio of IPA and SLC) the bilayer. Structural changes that occur in the bilayer due to the incorporation of IPA were further scrutinized by using fluorescence spectroscopy where extrinsic fluorescent probes 1, 6-diphenyl-1, 3, 5-hexatriene (DPH) and 7-hydroxycoumarin (7HC) were introduced. Variation in the crystalinity of the membrane as well as the head group packing with the composition could be correlated from the fluorescence spectroscopic analyses. Entrapment efficiency (E.E.) of the vesicles towards the cationic dye methylene blue (MB) was also evaluated. Morphological behaviours of the vesicles were successfully documented by TEM measurement and the results obtained, were also correlated with the size that obtained from DLS study.

## 2. Experimental Section

### 2.1. Materials

L-α-phosphatidylcholine (soylecithin, SLC, from soybean) was obtained from EMD Chemicals, Germany. A. R. grade sodium dodecylsulfate (SDS) [$CH_3(CH_2)_{11}SO_4Na$], hexadecyltrimethylammonium bromide (HTMAB) [$C_{16}H_{33}N(CH_3)Br$], 1,6-diphenyl-1,3,5-hexatriene (DPH), 7-hydroxycoumarin (7HC) and (3β)-cholest-5-en-3-ol (cholesterol) were the products of Sigma-Aldrich Chemicals Pvt. Ltd. (USA). A.R. grade disodium hydrogen phosphate ($Na_2HPO_4$, $12H_2O$), sodium hydrogen phosphate ($NaH_2PO_4.2H_2O$), sodium chloride (NaCl), methylene blue (MB) and chloroform (HPLC grade) were the products from Merck Specialities Pvt. Ltd, India. All the chemicals were stated to be more than 99% pure and were used as received. Double distilled water with a specific conductance 2-4 μS (at 25 $^oC$) was used for the preparation of solutions.

### 2.2. Methods

#### 2.2.1. Preparation and Isolation of IPA

Stoichiometric amount of aqueous HTMAB solution was added drop wise to a 0.1M aqueous solution of SDS under constant stirring. The white precipitate obtained, was extracted using chloroform.[18] Vacuum drying technique was introduced to remove the organic solvent. The white powder was then redissolved in chloroform and dried again. The process was followed for three cycles.[18] Fine white powders HTMA-DS (IPA) was then obtained and stored in vacuum desiccators.

#### 2.2.2. Preparation of Vesicles.

Small unilamellar vesicles (SUVs) were prepared by conventional thin film technique.[12,19] Molar ratio of SLC: IPA was set at 10:0, 9:1. 8:2. 7:3, 6:4 and 5:5 along with

30 mol% cholesterol. Quantitative amount of SLC, IPA and cholesterol were dissolved in chloroform in a round bottom flask followed by solvent evaporation in a rotary evaporator. Finally trace amount of solvent was removed by the stream of nitrogen ($N_2$). The thin film obtained was then rehydrated for 1h in PBS (0.1 M $Na_2HPO_4$, 0.1M $NaH_2PO_4$, 100mM NaCl, pH 7.4) at 70 $^oC$, well above the chain melting temperature of all the lipidic components. It was then frozen at −20 ºC and thawed in an ultrasonic water bath at room temperature for 15 min. Freeze-thaw process was repeated for another 4 cycles. Finally it was extruded using 0.45 μM cellulose nitrate membrane filter (Whatman Gmbh, Germany). Dye loaded vesicles were obtained by mixing appropriate amount of dye (DPH and 7-HC) into the lipid mixture before the generation of the thin film such that the final ratio of lipid and dye was 200:1. The total phospholipid concentration was kept at 2mM and was diluted depending on the type of experiment.

### 2.2.3. Surface pressure (π) – Area (A) Isotherm Measurement

Surface pressure (π) – area (A) isotherms were recorded with a Langmuir balance (M/S Apex Instrument Co. India, Model LB2000C) with a stated resolution of 0.01 $mMm^{-1}$. The trough and the barrier were made up of teflon (both hydrophobic and lyophobic) to avoid any contamination.[18] To prevent the entry of dust particles, a Plexiglass box was used which covered the stage and trough. The trough was filled with the PBS solution at pH = 7.4 with iconicity 100mM NaCl. A lipid monolayer film was formed by careful spreading of quantitative amount of the lipid ± IPA (with 30 mol% cholesterol) solutions dissolved in chloroform (1.0 $mgmL^{-1}$) with a Hamilton syringe (USA) onto the air-buffer interface. The solvent was allowed to evaporate approximately for 20min. Surface of the subphase was pre-cleaned using a micropipette aspirator, before spreading the monomolecular film. All the π – A isotherms were recorded at a subphase temperature of 25±0.5 $^oC$ with a lateral compression

rate of 5.0 mm $min^{-1}$. For each set of experiments, the curve was repeated at least twice to achieve the reproducible result. Further details are available in the literature.[20,21]

### 2.2.4. Dynamic Light Scattering (DLS) Studies

DLS studies were carried out to determine the hydrodynamic diameter ($d_h$), polydispersity index (PDI) and zeta potential (Z.P.) of different vesicle formulations.[16, 22] A dynamic light scattering spectrometer (Zetasizer Nano ZS90 ZEN3690, Malvern Instruments Ltd, U. K) was used for such studies. A He-Ne laser with an emission wavelength of 632.8 nm was used and all the data were recorded at a scattering angle of $90^0$. The translational diffusion coefficient (D) was actually measured by this instrument which is correlated with the diameter ($d_h$) of vesicles according to Stokes-Einstein's equation:[22]

$$d_h = \frac{kT}{3\pi\eta D} \quad (1)$$

where, k, T and η indicate the Boltzmann constant, temperature and viscosity of water respectively. Polydispersity index (PDI) is another informative parameter which could be obtained from the DLS studies. Zeta potential (Z.P.) values were measured using folded capillary cells. All the measurements were carried out at temperature 25 $^oC$ and each reported zeta potential value was an average of four measurements.

### 2.2.5. Transmission Electron Microscopy (TEM)

Synthesized vesicles with varying composition of SLC+IPA were prepared as described earlier. One drop of liposomal dispersion was placed on Formver™ carbon-coated 200mesh copper grid.[23] The excess drop was removed by using a piece of filter paper from the edge of the grid. The grid was then dried for 10 minutes before performing the measurement. The dry sample loaded grid was then viewed through Hitachi H-600

transmission electron microscopic (Japan) using the standard procedure. The voltage was set at 80KV.

### 2.2.6. Differential Scanning Calorimetry (DSC) Studies

DSC studies were performed to evaluate the chain melting temperature/phase transition temperature ($T_m$) and related thermodynamic parameters of the bilayer which eventually control the physical states of vesicles. Experiments were carried out in a Mettler Toledo differential scanning calorimeter (DSC 1, STAR$^e$ system, Switzerland). The dry thin films were rehydrated in 40 μL sealed Al pan. Each sample was scanned two times with a scanning rate 5 $^oC$ /min and 2 $^oC$ /min for complete heating and cooling cycles. The reference pan was sealed with PBS (pH 7.4). The obtained results were calculated by StarE software.

### 2.2.7. Fluorescence Spectroscopic Studies

Solvatochromic dye 7-HC and hydrophobic probe DPH were employed to investigate membrane polarity and bilayer packing respectively. Having some oxygeneous moiety, coumarine derivatives accommodate itself into the palisade layer of vesicles.[24] Overall membrane polarity was thus determined from the steady-state spectra of 7-HC comprising systems. The spectra were recorded by using a bench-top spectrofluorimeter (Quantummaster-40, Photon Technology International Inc., NJ, USA). Steady-state fluorescence spectra of 7-HC under different conditions were recorded in the range 350-600nm with an excitation wavelength of 330nm ($\lambda_{ex}$). Fluorescence anisotropy of 7-HC was determined by recording the emission data at 379 nm. Fluorescence anisotropy values for the probe embedded in the liposomal bilayer were obtained using the following equation:[25,26]

$$r = \frac{I_{VV} - GI_{VH}}{I_{VV} + 2GI_{VH}} \quad (2)$$

where, $I_{VV}$ and $I_{VH}$ were the fluorescence intensities, the subscripts indicate the position of the excitation and emission polarizer. G = $\frac{I_{HV}}{I_{HH}}$ was the grating correction factors. DPH, being a hydrophobic dye, is expected reside inside the bilayer.[27-29] Steady-state fluorescence anisotropy technique was employed to measure the membrane rigidity. All the anisotropy data were recorded at room temperature with excitation wavelength 351nm and the emission was set to 421 nm for DPH where as that for 7- HC, excitation and emission wave length were set to 330 nm and 379 nm respectively.

### 2.2.8. Entrapment Efficiency

Entrapment efficiency (E.E.) reveals the dye entrapment capacity of the vesicles. To determine the entrapment efficiency, lipidic components (SLC, IPA and cholesterol) were dispersed in PBS (pH 7.4) containing known amount of methylene blue (MB).[23] Three cycles of freeze-thawing technique, as mentioned earlier, was adopted so that the dye concentration inside and outside vesicle remained the same. 40μM MB loaded vesicles were made in such a way so that final concentration of lipid: MB becomes 50:1. MB loaded samples were centrifuged at 10, 000 rpm for 2h. The supernatant containing free MB molecules were analyzed in UV-visible spectrophotometer (Spectro UV-VIS double beam PC scanning spectrophotometer, UVD-2950, Labomed INC., USA) and the absorbance values were recorded for different sets of vesicles. The entrapment efficiency was calculated by using the following equation:[30]

$$\text{E.E. (\%)} = \frac{T-C}{T} \times 100 \qquad (3)$$

where, T is the total amount of dye presents both in the sediment and supernatant, C is the amount of drug detected only in the supernatant. T and C values were determined colorimetrically.

## 3. Results and Discussion

### 3.1. Surface Pressure (π) – Area (A) Isotherm

Using a Langmuir-Blodgett trough, pure and mixed lipidic monolayers were conveniently studied at the desired combination, which is otherwise not possible in the form of bilayer. Besides, different physicochemical parameters, *viz.*, molecular organization and subsequent interaction between the different components, limiting area, excess thermodynamic potential, film compressibility, *etc.*, were evaluated from such measurements.[18] Despite the fact that the monolayers effectively being only half a bilayer, with a flat rather than curved structure, information from the monolayer studies can effectively be translated into liposome or cell membrane systems.[31] With this background, surface pressure-area isotherms for SLC +IPA mixtures (in presence of 30 mol% cholesterol) were recorded at the air-PBS buffer (pH 7.4) interface. π-A isotherms for different combinations of SLC+IPA, along with 30 mol% cholesterol, have been shown in Figure 1. The limiting area appeared at 1.07 $nm^2molecule^{-1}$ for SLC while that for the IPA was at 1.08 $nm^2molecule^{-1}$. Results were found to be comparable with the previously published reports.[18,32] Monolayers with unsaturated lipid, exhibit as a single homogenous liquid expanded (fluid) phase.[17,20,32] The limiting area of IPA was found to be 1.08 $nm^2molecule^{-1}$ at zero surface pressure, that means, at the interface the limiting area per alkyl chain or in other words the half of the limiting area of an IPA was then about 0.54 $nm^2molecule^{-1}$; which was found to be larger than the theoretically proposed value, ~ 0.20 $nm^2molecule^{-1}$ per single chain.[20] This larger limiting value suggests that the molecular packing at the interface was somehow correlated to the bulky head groups of the IPA. Additionally, non-parallel orientations of the hydrocarbon chains were responsible for such differences. Cholesterol with a relatively smaller lift-off (0.3 $nm^2$) area has a propensity to interdigitize itself into the bilayers with parallel orientation.[17]

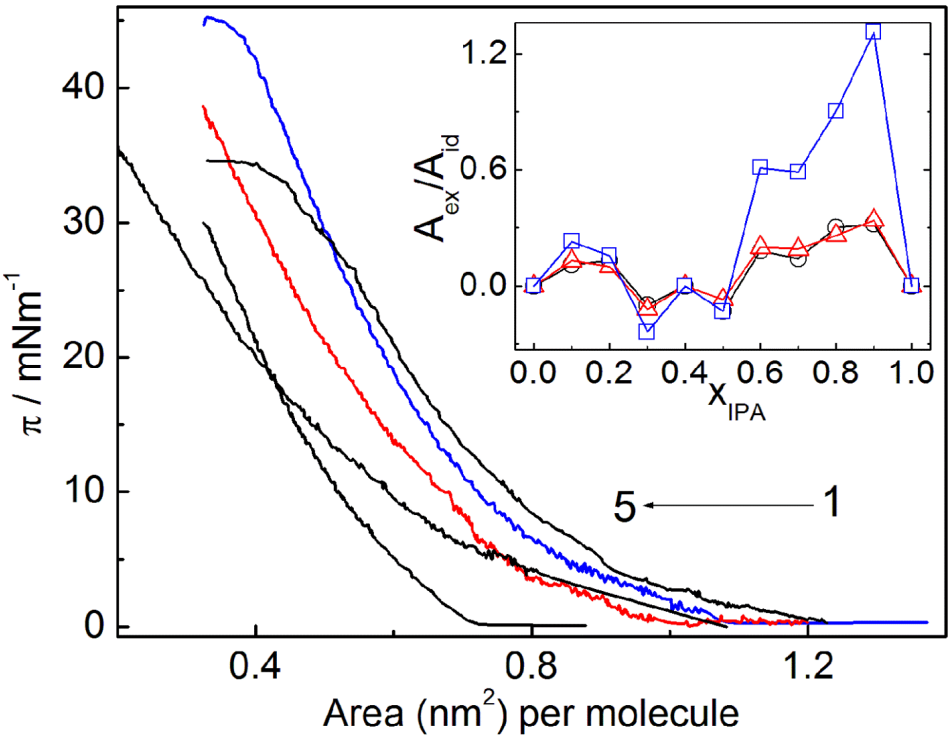


**Figure 1.** Surface pressure (π) – area (A) isotherm for the monomolecular films of SLC+IPA (in presence of 30 mol% cholesterol) at the air-buffer interface. Temp. 25 $^{o}$C. Mole fraction of IPA ($x_{IPA}$): 1,0.2; 2, 0.0; 3,0.4; 4,1.0 and 5,0.5. Inset: $A_{ex}/A_{id}$ *vs.* $x_{IPA}$ profile at π = O,0; Δ, 20 and □, 30 mNm$^{-1}$. A 0.1 mM PBS buffer (pH 7.4) in 100 mM NaCl was used as the subphase.

Isotherms of mixed monolayers ((SLC+IPA) were different from that of the individual components. Expanded isotherms were noticed for the systems with $x_{IPA}$ = 0.2; where the limiting area was found to be highest, 1.21 nm$^2$molecule$^{-1}$. Comparably condensed states for the mixed monolayer were initiated for $x_{IPA}$ ~ 0.3 and this trend followed upto 0.5. The isotherms for the mixed monolayers shifted to lower area region from that of the pure isotherms with gradual increment of IPA and indeed the limiting area was reduced from 1.21 nm$^2$ molecule$^{-1}$ ($x_{IPA}$ = 0.2) to 0.71 nm$^2$molecule$^{-1}$ where $x_{IPA}$ being 0.5 as estimated from the π – A isotherms. Such studies clearly indicate the renovation/reorganization of the molecular packing at the interface to a more condensed state when the IPA mole fraction was higher ($x_{IPA}$ > 0.2). The unusual variation in the lower mole fraction range of IPA can be

rationalized as follows: the Columbic forces of repulsion between bulky choline head groups of SLC were dominant in the presence of lower amount of IPA leading to the expanded (fluidic) monolayer. Increasing amountof IPA ( > 20 mol%) in the mixed monolayer, assist the hydrogen bonding or some sort of van der Waal's forces of attraction between SLC and IPA which overcome the columbic force exerted by the choline head groups, thus condensed mixed monolayer was resulted.

Da-Cheng et al.[32] reported that $C_8$- substituted alkylaminomethyl rutin (DAMR) and SLC were miscible but exhibit intermolecular repulsive force over the entire range of DMAR mole fraction. Reports on the monomolecular film studies in combination with different amphiphiles are available in the literature. Chang *et al*.[6] studied the monolayer behavior of IPA in presence of double tail cationic surfactant dihexadecyldimethylammoniumbromide (DHDAB), where the dissociation of the IPA was confirmed at $x_{DHDAB}$ = 0.5.[20] Characterization of IPA was further reported by Panda *et al*.[18] where solubilisation of IPA in presence of additives like cholesterol and bile salt were confirmed and the distinguished properties of IPA with the variation of alkyl chain length were observed. In all of their studies film functionality were found to be dependent on the composition of the lipid mixture.

Isotherms of the pure components lead to calculate ideal isotherms for the mixed systems according to additivity rule:[33]

$$A_{id} = x_1 A_1 + x_2 A_2 \quad (4)$$

where, $A_{id}$ is the average theoretical area per molecule, $x_1$ and $x_2$ being mole fractions of the components 1 (SLC+30 mol% cholesterol) and 2 (IPA+30 mol% cholesterol) respectively. $A_1$ and $A_2$ are the corresponding area per molecule for the individual components. Mixed monolayer which follow equation 5 were said to be ideal in nature. Deviation of the

experimental value ($A_{ex}$) from the ideal one can be obtained through the calculation of the excess area per molecule as:[21]

$$A_{ex} = A_{12} - A_{id} \quad (5)$$

where, $A_{12}$ is the experimental area per molecule of the mixed monolayer. Any deviation from linearity or any incidence of the appearance of maximum or minimum with varying composition would produce the extent of deviation from ideality.[34] In the case of an ideal mixture, the calculated value ($A_{id}$) should be equal to that of the measured value ($A_{12}$) and should vary linearly with mole fraction of any components. On the other hand, for immiscible/noninteractive systems, each component hangs about as individual/separate clusters containing substantial/considerable amount of molecules. A negative deviation from the ideal behavior signifies associative interaction between lipidic hydrocarbon chains and the IPA. While a positive deviation (positive $A_{ex}$) signifies repulsive interaction.[35] Representative plots for the variation of $A_{ex}/A_{id}$ with composition are shown in the inset of Figure 1.

Initial positive deviation (up to $x_{IPA}$ = 0.1 to 0.2) from the linearity was the outcome of repulsive interaction between SLC and IPA. Columbic repulsion which prevails at low $x_{IPA}$ causes the system to deviate positively from the ideality. However associative interactions were validating for the systems where $x_{IPA}$ were 0.3 and 0.5 respectively. Strong van der Waal's force of interaction along with some sort of hydrogen bonding results in the formation of associative type interaction which over crossed the Columbic repulsion for these systems. Significant divergence from the trend line was observed for $x_{IPA}$ 0.2 and 0.4, suggesting some anomalous interactions than other combinations. The calculated values of $A_{ex}/A_{id}$ for the former were found to be ~ 0.117 and that for the later was 0. This constancy was found for the entire range of surface pressure for the two. Loss of molecules from the monolayer into the subphase through the formation of vesicles and micelle could be the reason for this

peculiar behavior; as been reported by Chang *et al*.[6] Dissociation of $HTMA^+$ from IPA was the outcome when amphiphile concentration was higher and some sort of stress on IPA was initiated.[20] Accordingly, positively charged quaternary amine group of the zwitterionic choline moiety could exert strong electrostatic interaction with unbound $DS^-$ at the interface with the desorption of $HTMA^+$. $HTMA^+$, because of its reasonable water soluble characteristics, would not be able to withstand high surface pressure at interface after being dispatched by the choline moiety. Reports are supporting the fact that the dissociation of excess ionic surfactant from the mixed cationic/anionic monolayers with non equimolar ratio, whereas stably existed monolayer was confirmed with a mixture of equimolar ratio. Thus, it could be inferred that dissociation of $HTMA^+$ from IPA (HTMA-DS) was one of the reasons for the abnormal behaviour that generate excess area curve.

The condensation of mixed monolayer (area contraction) at higher $x_{IPA}$ was revealed form Figure 1 and the subtle structure of the monolayer could further be scrutinized from various factors such as ordering of chain, tilting of polar head and molecular packing. To obtain the state of the investigated film and the consequent molecular ordering, compression modulus was calculated (according to equation 6) for different mixed monolayers. Film compressibility ($C_s$) is a measure of the resistance of the monolayer against compression; in other words it can be defined as the amount of pressure needed to cause a change in the molecular area.[33] The reciprocal of compressibility,$C_S^{-1}$, known as compression modulus, is also another route to demonstrate the phase transition.

$$C_S^{-1} = -A\,(\delta\pi/\delta A)_T \qquad (6)$$

Such a representation is depicted in Figure 2. It is known that the monomolecular film with compressibility modulus in the range of 12.5- 50mNm$^{-1}$ are in the liquid- expanded (LE) phase, whereas for the liquid states the value lie in the range of 50-100 mNm$^{-1}$.[18]

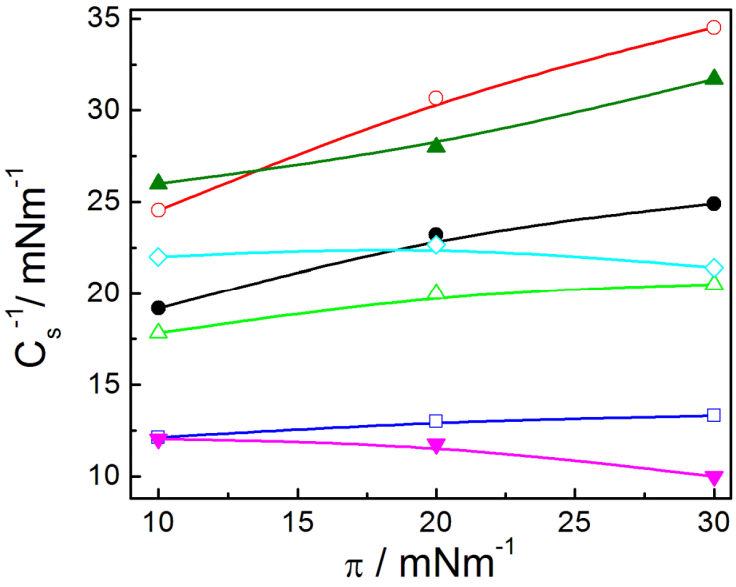


**Figure 2.** Variation in the compressibility modulii ($C_S^{-1}$) with the surface pressure for pseudo binary monomolecular films of SLC+IPA. A 30 mol% cholesterol was used. Temp. 25 $^{o}$C. Mole fraction of IPA ($x_{IPA}$): ●, 0; O, 0.1; Δ, 0.2; □, 0.3; ◊, 0.4; ▲, 0.5 and ▼ 1.0

In our present set of studies, all the mixed monolayers were in the LE phase as the compression modulus were in between 12.5 - 50 mNm$^{-1}$. $C_S^{-1}$ values were found to be larger for $x_{IPA}$ = 0.1 and little smaller for 0.5, which then increased with increasing surface pressure. Surface pressure independence of $C_S^{-1}$ was noted for the mixed monolayers comprising 20 and 40 mol% IPA which indeed was in good agreement with previous findings. Lowest $C_S^{-1}$ values were found for the system comprising 30 mol% IPA as well as the system comprising IPA alone. Because of the unsaturation, these monolayers were more compressible than their saturated analogue. IPA, with the acyl chain, being saturated, experienced less compressibility than SLC. Such an observation is not uncommon.

Mixed monolayer study could be useful to formulate stable liposomal dispersions by considering different thermodynamic parameters of the interaction processes. The spontaneity that associated with hydrophobic interactions between the hydrocarbons chains of SLC–IPA

can also viewed by evaluating the excess free energy change as given the following equation:[31]

$$\Delta G_{ex}^{0} = \int_{0}^{\pi} (A_{12} - A_{id})\, d\pi \qquad (7)$$

Quantitative assessment of the magnitude of the mutual interaction between SLC and IPA could be best studied by considering $\Delta G_{ex}^{0}$ values. Figure 3 describes the variation in the excess free energy with the composition of the mixed monolayer ($x_{IPA}$).

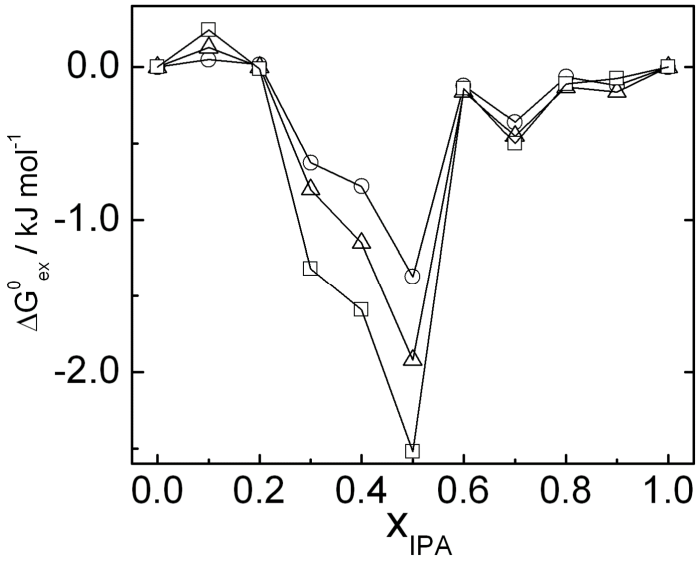


**Figure 3.** Variation of excess free energy ( $\Delta G_{ex}^{0}$) for the SLC+IPA mixed monolayer systems (in presence of 30 mol% cholesterol) with the mole fraction of IPA ($x_{IPA}$) at different surface pressure (mNm$^{-1}$) : O, 10 ; Δ, 20 and □, 30. Temp. 25 $^{o}$C.

Non ideal mixing behaviour between SLC and IPA was confirmed from the run of the curves; positive deviation from the ideal behaviour was observed for the system comprising < 20 mol% IPA. Columbic force of repulsive interaction between the polar head groups and the dissociation of $HTMA^{+}$ from IPA could be associated in the process of mixing. Again the cis orientation of one of the fatty acyl chains of SLC could resist the IPA to get condensed and subsequent non spontenity in the mixing processes were observed. Negative values of

$\Delta G_{ex}^{0}$ for $x_{IPA}$ = 0.3, 0.4 and 0.5 indicate that the supplement of IPA into SLC monolayer grounds the formation of stable monolayer at their favourable arrangement. Because of the saturation of IPA, strong van der Waals force of interaction and hydrogen bonding among SLC and IPA result in an associative manner. Thus stable mixed monolayer was resulted at higher mole fraction of IPA. Unlike the systems with 30 and 50% IPA, monolayer with 40 % IPA did not follow the same trend and produced relatively lower negative value of $\Delta G_{ex}^{0}$ compared to the other two. Unfavorable interaction between SLC and IPA could be the reason as $HTMA^{+}$ has a propensity to dissociate (when $x_{IPA}$ is higher) in the presence of quaternary ammonium ion of the choline group and get solubilised into the subphase. Thus the small negative $\Delta G_{ex}^{0}$ that originate for the system with 40% IPA could be due to the associative electrostatic interaction between ammonium ion and $DS^{-}$.

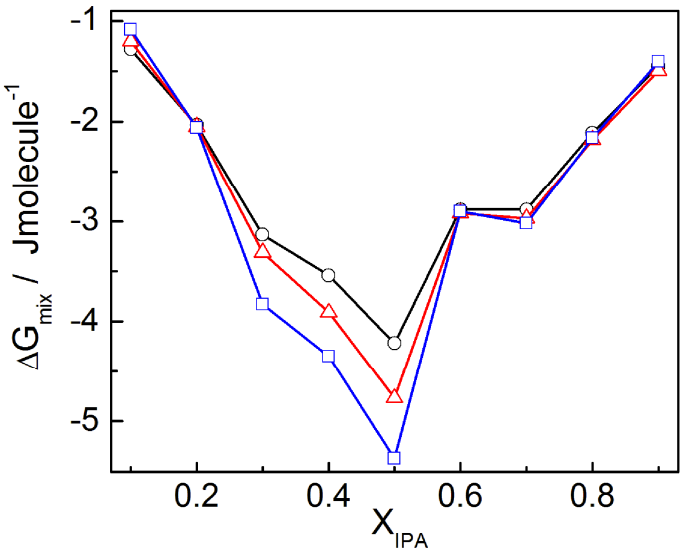


**Figure 4.** Variation of $\Delta G_{mix}$ as a function of composition for mixed monolayers of SLC+IPA at 25 °C. Surface pressures ($\pi$ / $mNm^{-1}$) are: O, 10; Δ, 20 and □, 30.

The extent of hydrocarbon chain mixing among SLC and IPA was further calculated in terms of free energy of mixing ($\Delta G_{mix}$). Figure 4 illustrates the free energy of mixing for the mixed monomolecular film of SLC and IPA as a function of IPA mole fraction.

In order to further scrutinize the interaction between SLC and IPA in their monolayer forms, apart from conventional monolayer thermodynamic parameters, regular solution theory was adopted. Interaction parameter (I. P.) describes the extent of interaction between SLC and IPA in mixed monolayer state and can be derived by using following equation:[32]

$$\text{W} = \frac{\Delta G_{ex}^{0}}{x_1 \, x_2} \tag{8}$$

$$\text{I.P.} = \frac{W}{RT} \tag{9}$$

I. P. as a function of π was plotted in Figure 4 and shows some fascinating points regarding the interaction process. Figure 5 indicates that interaction was maximum for $x_{IPA}$ = 0.1 and increasing linearly with π, whereas that for $x_{IPA}$ = 0.3 and 0.4, I.P. independence of mixing on the surface pressure for the system comprising 20 mol% IPA was further established through its parallel propagation along the X- axis. Relatively high extent of interaction for $x_{IPA}$ = 0.1, was due the presence of least amount of IPA in the monolayer. Presence of one IPA molecule for nine other combinations was a state where IPA was assumed to be interdigited by huge amount of SLC. Cholesterol, being an additive, played an important role for the interaction process. With increasing π, cholesterol pushes the acyl chains of SLC which in turn hold the saturated hydrocarbon chain of IPA firmly to produce reasonable I.P. for this mixed monolayer. It could be stated as "arresting the IPA by lipids assembly through the lipophilic solvation in monolayer". On the contrary, we noticed relatively lower I.P. values for the systems with higher proportion of IPA. To address the corollary, one must need to consider the influence of head group packing between SLC and IPA. It is now been known that IPA constitutes bulky head groups which produce lesser tight packing when mixed with SLC (as choline group is also a bulky head group). Again desorption of $HTMA^+$ from IPA and its subsequent solubilisation was the reason that we could not find any changes in the values of I. P.

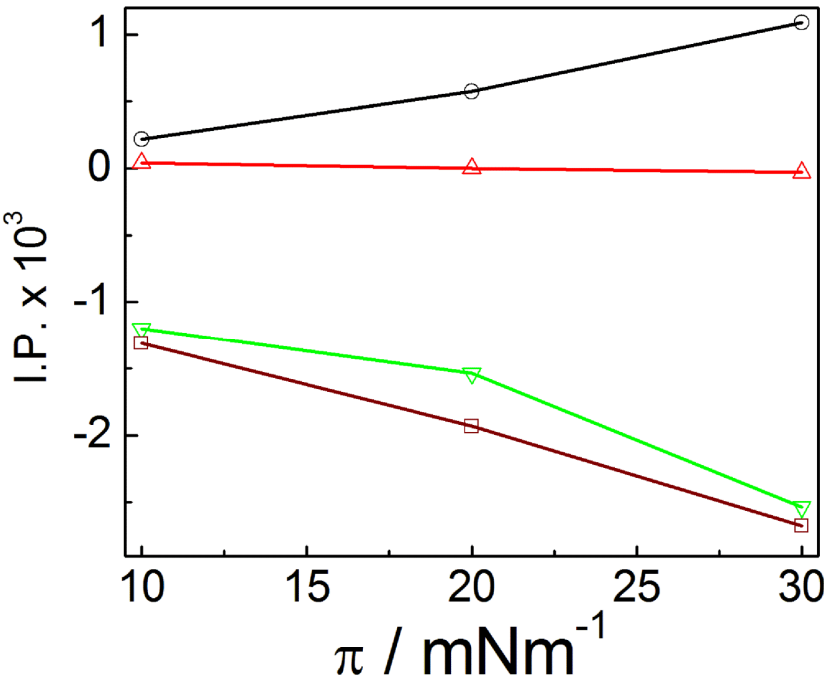


**Figure 5.** Relationship between interaction energy (I. P.) and surface pressure (π) at different IPA mole fraction. $x_{IPA}$: ○, 0.1; Δ, 0.2; ∇, 0.3 and □, 0.4. Temperature was set on 25 $^{o}$C.

Lipid assemblies in the monolayer and bilayer forms are different. While the former having linear orientation that for the later show curvature. Although there are some structural differences, mixed monolayer studies could be informative to explain the stability and biodiversity of SLC-IPA vesicles. It was concluded from π – A study that increasing proportion of IPA made the system more rigid although 10 mole % of IPA exhibited repulsive interaction. Some aberration for 20 and 40 mol% of IPA were observed. Such anomalous behaviours are beyond explanation with the present level of knowledge. The mechanisms of such interactions are yet to be cleared and could be explained on the basis of molecular dynamics simulation which is considered as one of the future perspectives.

### 3.2. Dynamic Light Scattering (DLS) Studies

Hydrodynamic diameter ($d_h$) is an important parameter towards the direction of stability and bio distribution of vesicle formulations. Apart from the size, polydispersity index (PDI) is considered to be another important parameter as it describes the size distribution of dispersions having range from zero for a monodispersed system upto unity for completely polydispersed systems. Stability of the vesicles with different compositions of SLC and IPA, in combination with 30 mol% cholesterol, was investigated through the size measurement for a time period over 100 days starting from the day of sample preparation. Representative sizes vs. time (day) profiles are presented in Figure 6. Some important information could have been achieved from such plots. Size of the vesicles passed through a minimum at ~ 10 – 12 days (except the system with $x_{IPA}$ = 0.2), which depended on the composition. This time period may be viewed as the equilibration time for the vesicles. Flipping and reorganization of liposomal components occurred during this time period which led to the decrease in size. Initial observation shows that progressive addition of IPA to the SLC resulted in the size increment of vesicles. System comprising 40 mol% IPA exhibited completely different behaviour. Additionally it was observed that the equilibration time increased with increasing mole fraction of IPA. Initial size contraction for equilibration (for $x_{IPA}$ = 0.1, 0.2 and 0.3) may be attributed to the presence of saturated hydrocarbon chain of IPA which produces more hydrophobic environment in the bilayers. However permanent size contraction was involved for the liposome with $x_{IPA}$ = 0.1, as also reflected from highest $C_S^{-1}$ and I. P. (shown earlier) that demonstrate the strong interaction between SLC and IPA. Vesicles with 30 and 50% IPA showed exceptional stability upto 100 days; the spontaneity of the interaction that arise for these two systems, as revealed from the excess Gibbs potential ($\Delta G_{ex}^0$) value from monolayer study, also support the fact. Size of the vesicles with $x_{IPA}$ = 0.2 and 0.4 monotonously increased with time; such systems also exhibited relatively higher PDI

value. Such a different behavior could be rationalized through the surface pressure independent repulsive interaction between SLC and IPA as already reflected from the monolayer studies. Dissociation of $HTMA^+$ from IPA could lead unfavourable orientation for lipid acyl chain which could lead the way of destabilization. However the modes of interactions for these two sets of vesicles are yet to be revealed and cannot be explained with the present level of knowledge.

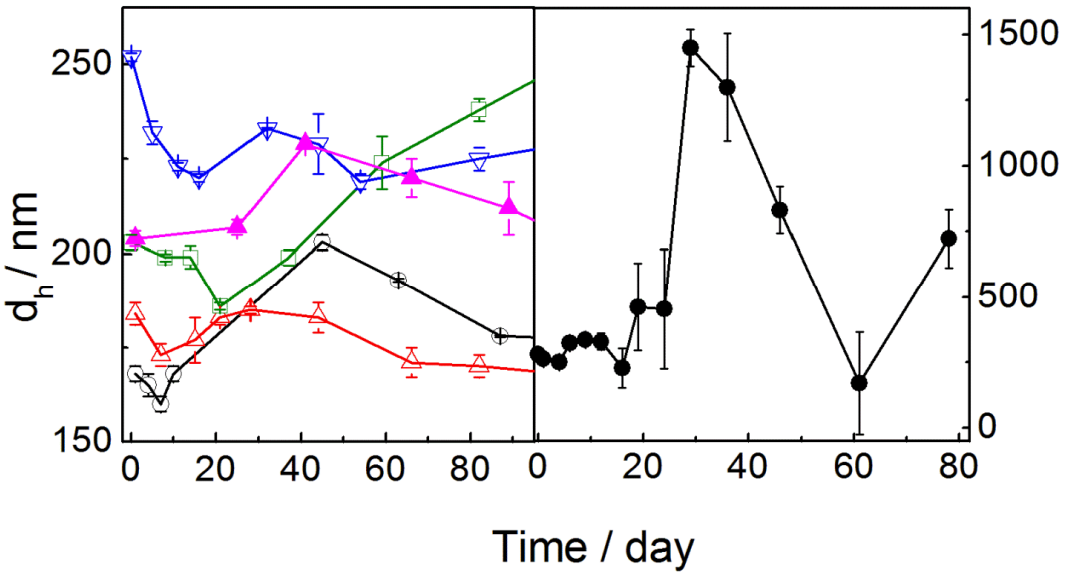


**Figure 6.** Variation in the hydrodynamic diameter ($d_h$) for SLC +IPA (in presence of 30 mol% cholesterol) vesicles with time at 25 $^oC$. Mole fraction of IPA ($x_{IPA}$): O, 0; Δ, 0.1; □, 0.2; ∇, 0.3; ▲ ,0.5 and ●, 0.4

Change in the PDI values with time have been graphically presented in Figure 7. Results on the DLS data recorded day 45 are shown in Table 1 as representative. Stable liposomal dispersions were formed for the systems with the following compositions of SLC/IPA (M/M): 10:0, 9:1, 7:3 and for 5:5. $d_h$ – time profile for the different systems have been graphically presented in Figure 6. Addition of IPA (except $x_{IPA}$ = 0.4) resulted in the decrease in polydispersity which remained almost constant with time.[36] It could therefore be

concluded that the IPA plays an important role in stabilizing the vesicles by imparting monodispersity for which the IPA could be considered as novel substitutes of the conventional phospholipids.

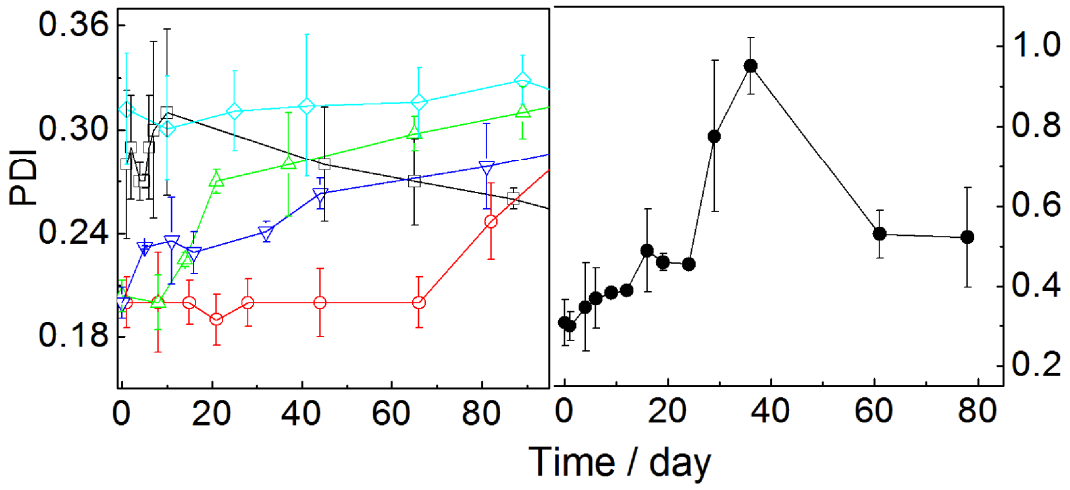


**Figure 7.** Variation of polydispersity index for the SLC+IPA (in presence of 30 mol% cholesterol) vesicles with time. Mole fraction of $x_{IPA}$: □, 0; O, 0.1; Δ, 0.2; ∇, 0.3; ●, 0.4 and ◊, 0.5.

Zeta potential (Z. P.) is another major parameter that holds the physical stability and subtle structure of vesicles as it determines the electrostatic repulsion between the vesicles.[12] Table 1 represents the zeta potential of the vesicles with different SLC+IPA molar ratio recorded on day 45 of the sample preparation. Generally the zeta potential values were found to be negative, which accounts for the electrostatic stabilization among the lipidic dispersion and thus prevent vesicles from fusion or aggregation (the mean size did not change much as reflected from hydrodynamic size measurement study). With gradual increasing proportion of IPA in the vesicles (with respect to SLC), negative zeta potential values moved towards the positive range. SLC, a naturally occurring phospholipid exhibited Z.P. ~ −20.7 mV. The negative value of Z. P. was found to decrease with increasing IPA mole fraction. Variation of Z.P. with composition was non linear and followed two degree ($2^0$) polynomial equation with $R^2 = 0.95$.

**Table 1.** Hydrodynamic diameter ($d_h$), Zeta potential (Z. P.) and Polydispersity index (PDI) values for the different vesicle formulations at 25 $^oC$. Values correspond to the data acquired on day 45 of the sample preparation

| SLC:IPA | $d_h$ / nm | Z. P. /mV | PDI |
|---|---|---|---|
| 10:0 | 203.0±2 | -20.7± 1.41 | 0.28 ± 0.03 |
| 9:1 | 182.4±4 | -7.17 ± 1.30 | 0.20 ± 0.02 |
| 8:2 | 207.8±2 | -1.59 ± 0.45 | 0.28 ± 0.03 |
| 7:3 | 227.8±8 | -1.53 ± 0.79 | 0.24 ± 0.006 |
| 6:4 | 877.5±89 | +3.02 ± 0.87 | 0.95 ±0.07 |
| 5:5 | 228.4±1 | -1.71 ± 1.41 | 0.31 ± 0.04 |

Although we could prepare vesicles with 40 mol% IPA which showed positive zeta potential, however was certainly a discrepancy that was due to the dissociation of $HTMA^+$ from IPA. The dispatched $HTMA^+$ into the aqueous medium resulted in the formation of some micelle like structure which pushed the Z. P. in the positive range. The instability of the vesicle having $x_{IPA}$ = 0.4 now could well be realized and could be correlated from the monolayer studies.

### 3.3. Transmission Electron Microscopy

Both normal TEM and freeze fractured TEM (FF-TEM) studies were carried out with an aim to confirm the formation of vesicles as well as their morphologies[37-40,21,30,31,44] also the impact of IPA on vesicles size could be evidenced from such measurements.[37,38,21,44,42] Representative TEM image of the vesicle with 30 mol% IPA has been shown in Figure 8. Spherical morphology and bilayer structure of the vesicles were confirmed from the image. In

the inset, the magnified image of the selected vesicle further revealed the existence of the bilayer.

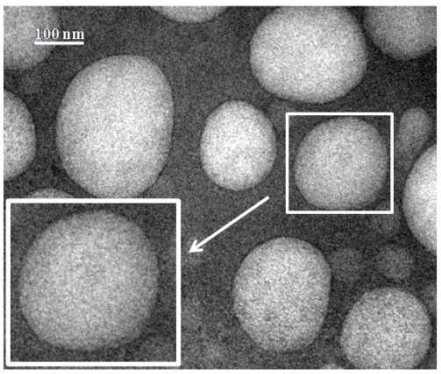


**Figure 8.** Representative TEM image of SLC+IPA (7:3, M/M) vesicles. Inset: Magnified image of the selected area. Scale bar is indicated in the figure.

Thus TEM measurement could be considered as a useful tool to characterize a vesicular system. FF-TEM studies were carried out to further support the normal TEM measurements, presented in Figure 9 as representatives.[39-41] Both the images in panel A (pure SLC) and B (7:3 SLC+IPA system) put on a view of spherical morphology as well as bilayer section around the vesicles. A distinct bilayer structure could be visualized as shown in the inset of panel A.

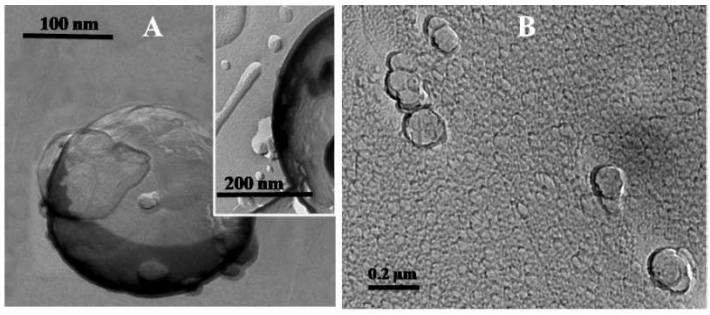


**Figure 9.** Freeze fractured TEM images of SLC+IPA (10:0, M/M, panel A) and SLC+IPA (7:3, M/M, panel B) vesicles. Scale bars are indicated in each panel.

Vesicle sizes were found to be comparable in both normal TEM and in FF-TEM. Impact of IPA on SLC bilayer have been explored by means of different instrumentation, like DLS study; the fate of the vesicles were found to be same here also as we have witnessed minor size enhancement for 7:3 SLC+IPA. Spherical morphology of the vesicles was confirmed from the images and the clustered form so obtained was not uncommon for the vesicular systems.

### 3.4. Differential Scanning Calorimetry (DSC) Studies

Chain melting temperature ($T_m$) of the bilayer dispersion, its crystalinity, enthalpy of the transition processes ($\Delta H$) as well as the heat capacity values ($\Delta C_p$), *etc.*, can suitably be evaluated by DSC studies. Such studies are exceedingly responsive in presence of exogenously added compounds (herein the IPA).[37] Exogenously added compound may alter the half peak width ($\Delta T_{1/2}$). In the present set of studies, DSC measurements were carried out in the temperature range $-25$ to 25 $^{o}$C with a scan rate of 2 $^{o}$C min$^{-1}$. Representative thermograms are shown in Figure 10. Vesicles of different compositions with 30 mol% of cholesterol generated three distinct separate events. Two endotherms appeared at "a" in the temperature range $-20$ to $-19$ $^{o}$C and another and "c" in the temperature range 3 to 6 $^{o}$C respectively. The exothermic one, "b" appeared in the temperature range 0 to 3 $^{o}$C. SLC, with an unsaturation in one of its fatty acyl chains, exhibited the $T_m$ at around $-20$ $^{o}$C .The value was found to be comparable with the previously published report.[42] Endotherm "a" was due to the 'phase transition' or 'chain melting' of mixed acyl chains of SLC.[42] IPA has discrete effect on the thermograms. The bilayer chain melting temperature ($T_m$), width at half-peak height ($\Delta T_{1/2}$),[43] enthalpy change ($\Delta H$) and corresponding heat capacities ($\Delta C_p$) for the different formulations have been summarized in Figure 11.

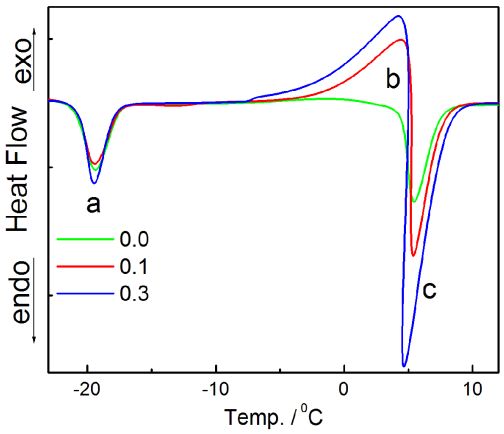


**Figure 10.** DSC thermograms of SLC+IPA vesicles at different SLC/IPA ratio (in presence of 30 mol% cholesterol). Scan rate: 2 $^{o}$C min$^{-1}$. Mole fractions of IPA are mentioned inside the figure.

Incorporation of 10 mol% IPA enhanced $T_m$ (0.8%) and lowered the $\Delta T_{1/2}$ (1.3%) values at ~ −20 $^{o}$C mildly, but a significant increase in the negative value of $\Delta H$ (11%) and positive value of $\Delta C_p$ (16%) were noticed. It was found that progressive addition of IPA into the SLC bilayers decreased the $\Delta T_{1/2}$ while increased $\Delta C_p$ in the transition region marked as 'a". Sequential decrease of $\Delta T_{1/2}$ may be rationalized on the basis of the phase transitions. Results further support the surface pressure-area isotherm derived data. In case of the system with 10 mol% IPA, the monolayer exhibited more rigidity. Addition of IPA can cause the increased crystalinity for which there occurred an increase in the transition temperature and decreased $\Delta T_{1/2}$ values.

IPA produced extra hydrophobic environment in the bilayers, which caused the physical state of bilayers as with its progressive addition turn the bilayers from fluid-phase to liquid crystalline phase. Because of the most ordered orientation of acyl chains in 5:5 SLC+IPA, it produced narrower distribution curve for the phase transitions. Increasing $\Delta C_p$ with increased concentration of IPA for SLC+IPA vesicles also further support the

aforementioned explanation which is also further established by steady state fluorescence anisotropy experiment with DPH as hydrophobic probe (to be shown later).

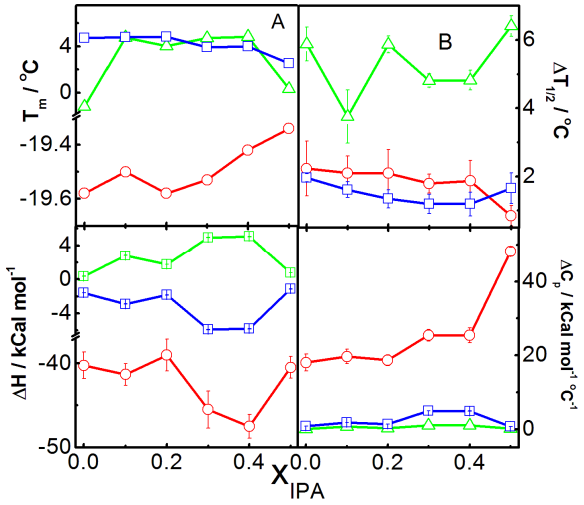


**Figure 11.** Variation in the transition temperature ($T_m$), half peak width of the transitions ($\Delta T_{1/2}$), and enthalpy changes for the melting ($\Delta H$) and changes in the heat capacity ($\Delta C_p$) with the composition ($x_{IPA}$) for SLC+IPA vesicles comprising 30 mol% cholesterol. PBS buffer at pH=7.4 was used in the preparation of vesicles.

The exothermic event 'b' was an outcome of IPA effect, as reflected from Figure 10. With increasing IPA concentration, heat change of the process was noticeably increased. This release of heat was due to the some sort of arrangement/packing of water molecule around the vesicles, which was a direct effect of IPA. Formation of an overlayer of water molecules over the lipidic head groups produces some sort of packing at temperature around 4 $^{o}$C, where the density of water was supposed to be highest. $T_m$ for 10:0 SLC+IPA was found to be −1.17 $^{o}$C, which interestingly jumped up to 4.76 $^{o}$C for 9:1 SLC+IPA and did not change much for 7:3 SLC+IPA. So it can be concluded that shifting of $T_m$ from −1.17 to 4.76 $^{o}$C was surely the IPA induced effect. Lower $\Delta T_{1/2}$ values for 9:1 and 7:3 SLC+IPA systems than 10:0 SLC+IPA indicate better packing of the hydrophilic overlayer as well as lipidic head

groups. This was again confirmed from the heat release (ΔH) of the process, where greater heat release for 9:1 and 7:3 SLC+IPA rather 10:0 were observed.

Appearance of neighbouring endotherm 'c' was a reverse consequence of the event 'b' where heat was absorbed. From the Figure 10 it was evident that the absorption of heat was also an IPA effect and exactly the opposite phenomenon to that of the exotherm 'b'. Endotherm 'c' was due to the disorganization of water overlayer surrounding the vesicles. At relatively higher temperature, the lipidic head groups were supposed to be vibrating. This vibration transforms the water overlayer to turn from an organized to disorganized states. Although the $T_m$ for 10:0, 9:1 and 7:3 SLC+IPA were not changed significantly, however relatively sharp peaks were noticed for the 9:1 and 7:3 SLC+IPA systems indicating better head group packing. Higher negative heat changes associated with 9:1 and 7:3 SLC+IPA systems again support the higher order of packing. It is now been known that both the events 'b' and 'c' were the two opposite phenomenon and expected to show reverse heat change as also reflected from the Figure 11.

### 3.5. Fluorescence Spectroscopic Studies

Fluorescence spectroscopy is another important technique which enables to explore the subtle structure of the membrane. Packing of bilayer (in the core of the membrane) and interaction of head groups (at the palisade layer) are the two major parameters for the formation of stable vesicle. With an aim to understand the packing of head groups, fluorescence spectroscopic studies were carried out using 7-hydroxy coumarin (7-HC) as a molecular probe. 7-HC is well known as a solvatochromic dye and has a great tendency to stay on the palisade layer of the membrane.[24] Emission spectra of 7-HC in solvents of different polarity were carried out as the references in order to understand the state of polarity

of the probe at the membranous interface. Emission spectra 7-HC in the vesicles of different compositions were recorded and compared with that in the solvents of different polarities.

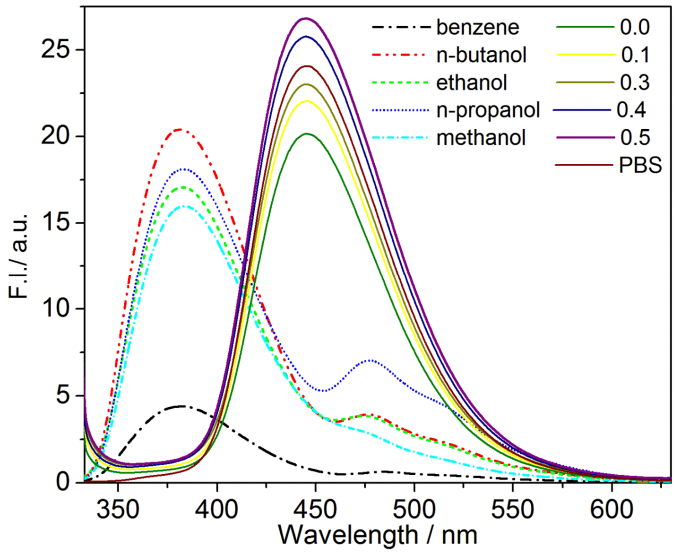


**Figure 12.** Fluorescence spectra of 10 μM 7HC in solvents of different polarity (dashed lines) and vesicles of varying composition (solid lines) at 25 $^{o}$C. Excitation wavelength ($\lambda_{ex}$) = 330 nm. Different solvents and the mole fraction of IPA are mentioned inside the figure. Spectra was also recorded in PBS alone

Emission spectra of 10 μM 7-HC under various conditions have been graphically presented in Figure 12. Periodic declinations of intensities along with a mild red shift were observed with increasing solvent polarity. Such an observation was also reported by others.[44] While considering the spectral behaviour of 7-HC in the vesicles of different compositions, it was observed that with increasing amount of IPA in the vesicles, fluorescence intensity was enhanced along with a mild blue shift. With increasing amount of IPA the difference in polarity was thus confirmed. It is not unexpected that IPA bearing neutralized head groups will effectively result in decreasing polarity of the bilayer. Another interesting thing that additionally comes into the picture is the polarity of SLC vesicles with variant mole fractions

of IPA. Results clearly indicate that with increasing amount of IPA in the vesicles, there were increase in rigidity and decrease in the polarity of the membranous interfaces.

.

With an aim to understand the packing of the hydrocarbon chains (inside the bilayer) similar studies were carried out using l,6-diphenyl-l,3,5-hexatriene (DPH) as the molecular probe. DPH being completely hydrophobic will preferentially reside in the lipid acyl chain with parallel orientation. Emission spectra of DPH in different vesicles have been shown in Figure 13. No significant change in the fluorescence spectra of DPH in different vesicles further supported its residence in the bilayer core. Results clearly indicate no change in the polarity of the core of bilayer for different combinations. However, the change in the hydrocarbon chain packing was further investigated by measuring the fluorescence anisotropy values.

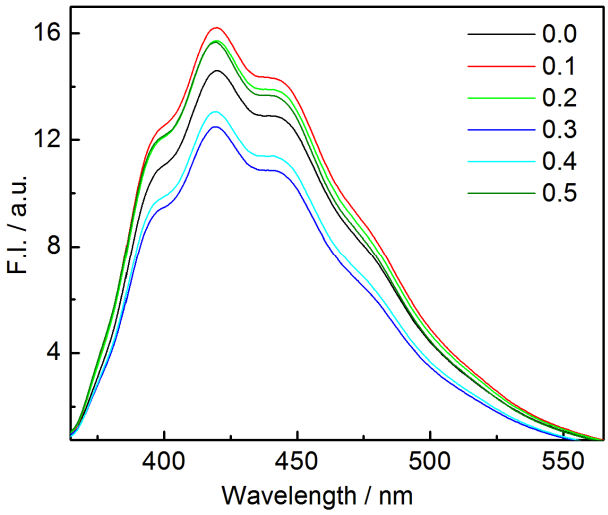


**Figure 13.** Fluorescence spectra of 10 µM DPH in PBS buffer (pH 7.4) in vesicles of varying composition at 25 $^{o}$C. Excitation wavelength ($\lambda_{ex}$) = 357 nm. Mole fraction of IPA are mentioned inside the figure.

Variations in the fluorescence anisotropy (r) with the composition of the vesicles ($x_{IPA}$) have been graphically presented in Figure 14.

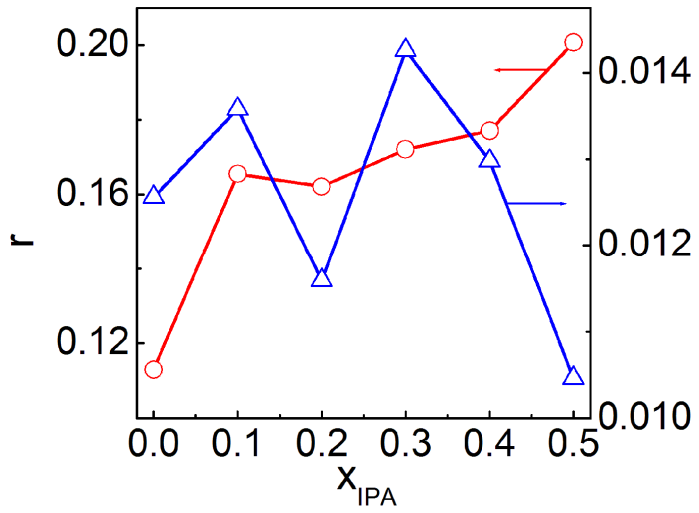


**Figure 14**. Variation in the fluorescence anisotropy (r) for DPH (O) and 7-HC (Δ) with the mole fraction of IPA ($x_{IPA}$) in the vesicles comprising SLC+IPA + 30 mol% cholesterol. Temp. 25 $^{o}$C. While DPH evaluates the anisotropy value for the core hydrocarbon region of the bilayer, 7-HC monitors the anisotropy of the palisade layer.

While considering the fluorescence anisotropy variation of 7-HC with $x_{IPA}$, it was noted that the addition of IPA resulted an initial increase in the 'r' values followed by the appearance of a maximum. Anomalous behaviour for the system comprising 20 mol% IPA was noticed. Such anomalous behaviour was also evidenced in other measurements. Initial increment of anisotropy was due to IPA addition which forced the SLC head groups to come closer. Such an incidence was most significant in case of 30mol% IPA. Lower anisotropy value for 5:5 SLC+IPA favours repulsive forces which cause the brakeage of head group packing. Unusual behaviour for the 20% IPA system clearly indicates non-favourable packing between the components. However, further studies, *viz*., NMR, small angle neutron scattering (SANS), small angle x-ray scattering (SAXS) and molecular dynamics simulation studies could shed light in such case, which are considered as the future perspectives.

Figure 14 also represents periodic increment in the anisotropy value with progressive addition of IPA for the systems comprising DPH as the molecular probe. Vesicles with pure

SLC showed lowest value because of the fluidic nature of the membrane. However progressive addition of IPA resulted in the rigidity enhancement of hydrocarbon chains which brought some sort of crystalinity into the bilayer. Such an observation clearly implies that one can appreciably control the physical properties of vesicles through the incorporation of IPA into the SLC bilayer.

### 3.6. Entrapment Efficiency

Entrapment efficiency (E. E.) of the vesicles with varying mole fraction of IPA has been tabulated in Table 2. E. E. was determined for the vesicles with varying composition. It was found that the E. E. was dependent on IPA concentration and satisfactory results were found through all the vesicles comprised with different mole fraction of IPA. Anomalous behaviour was noticed for the system having 40% IPA.

**Table2.** Entrapment Efficiency (E. E.) of Different Sets of Vesicles with Varying Mole Fraction of SLC and IPA. Temperature 25 $^{o}$C

| System | Entrapment Efficiency (%) |
|---|---|
| 10:0 SLC+IPA | 92.5±1.41 |
| 9:1 SLC+IPA | 90.0±1.30 |
| 8:2 SLC+IPA | 88.7±0.45 |
| 7:3 SLC+IPA | 79.2±0.79 |
| 6:4 SLC+IPA | 96.5±0.87 |
| 5:5 SLC+IPA | 53.9 ±1.41 |

The dye methylene blue is cationic in nature and expected to bind with the vesicles having negative surface potential. Pure SLC vesicles with highest negative zeta potential, showed maximum E.E. (92.50%) due to the strong electrostatic force of attraction. Progressive addition of IPA into the bilayer although decreased the E.E. mildly, yet the results were still reasonable as per as E.E. was concerned. 96.50% of E.E. was a strange result for $x_{IPA}$ 0.4, and it was possibly due to the dissociation of IPA into corresponding cationic ($HTMA^+$) and anionic ($DS^-$) parts. Presence of zwitterionic choline head group and anionic $DS^-$ could provide excess electrostatic force of attraction which leads to the high E. E. value.

**4. Conclusion**

SLC and IPA (HTMA- DS) in different mole fractions were used to prepare stable vesicles dispersions. Through the comprehensive investigation on the impact of IPA on the vesicles were studied from monolayer studies and it could be concluded that IPA exerts prominent influence on SLC monolayer. Associative interactions were found for some mixed monolayer however the systems with $x_{IPA}$ ~ 0.5 did not response to produce stable vesicles dispersions. Some aberrations were noted with the systems comprising 20 and 40 mol% IPA. Dissociation of $HTMA^+$ from IPA resulted in such unusual variation. This was further scrutinized by measuring the hydrodynamic size of the hybrid vesicles and we found relatively less stable vesicular dispersions for $x_{IPA}$ = 0.2 and 0.4. Polydispersity index values drew much attention because it unleashed the usefulness of IPA that reduce the PDI value and maintained fairly monodispersed system. TEM images of vesicles put on a view of spherical vesicular system and were well correlated to the data that obtained from DLS measurements. Packing of head groups as well as packing of the hydrocarbon chains were investigated through the combined DSC and fluorescence spectroscopy analysis where gradual incorporation of IPA into the bilayer produces rigidity or crystalinity. Systems comprising 0, 10, 20, 30 and 50 mol% IPA produce promising drug entrapment efficiency.

Thus IPA assisted vesicular system could be used as a carrier for drug delivery. The future prospective would be to characterize the system theoretically based on molecular dynamics simulation and to study the interaction through $^{1}H$, $^{13}C$ NMR, SANS and SAXS study.

**References:**

References are given in BIBLIOGRAPHY under Chapter I (pp. 151-153).